

Brain-Inspired Efficient Pruning: Exploiting Criticality in Spiking Neural Networks

Anonymous submission

Abstract

Spiking Neural Networks (SNNs) have been an attractive option for deployment on devices with limited computing resources and lower power consumption because of the event-driven computing characteristic. As such devices have limited computing and storage resources, pruning for SNNs has been widely focused recently. However, the binary and non-differentiable property of spike signals make pruning deep SNNs challenging, so existing methods require high time overhead to make pruning decisions. In this paper, inspired by critical brain hypothesis in neuroscience, we design a regeneration mechanism based on criticality to efficiently obtain the critical pruned networks. Firstly, we propose a low-cost metric for the criticality of pruning structures. Then we re-rank the pruned structures after pruning and regenerate those with higher criticality. We evaluate our method using VGG-16 and ResNet-19 for both unstructured pruning and structured pruning. Our method achieves higher performance compared to current state-of-the-art (SOTA) method with the same time overhead. We also achieve comparable performances (even better on VGG-16) compared to the SOTA method with 11.3x and 15.5x acceleration. Moreover, we investigate underlying mechanism of our method and find that it efficiently selects potential structures, learns the consistent feature representations and reduces the overfitting during the recovery phase.

Introduction

Spiking Neural Networks (SNNs) have garnered increasing attention (Wu et al. 2019; Zheng et al. 2021) as the third generation of neural networks (Maass 1997) in recent years. By emulating accumulation-excitation and event-driven behavior characteristics of biological neurons, SNNs have been an attractive option for deployment on devices with limited computing resources with lower power consumption compared to Artificial Neural Networks (ANNs) (Akopyan et al. 2015; Roy, Jaiswal, and Panda 2019; Davies et al. 2018; Pei et al. 2019). However, the limited computing and storage capacity causes a challenge to the implementation of SNNs on these devices, as the deep SNNs with large-scale parameters cannot be directly performed.

Network pruning provides prospect of reducing the computing and storage overhead. Researchers have made a lot of efforts on the unstructured pruning of SNNs. Some works are inspired by the human brain. (Kundu et al. 2021) mod-

eled the synapse regeneration process, while (Qi et al. 2018) designed a connection gate to prune synapses during training. (Kappel et al. 2015) modeled synaptic plasticity and spine motility to optimize network structure and connections. Recent researches on SNN pruning more reference with the techniques used in ANN pruning. Some works used predefined thresholds to remove weak weights of the model in the learning process (Neftci et al. 2016; Liu et al. 2019). (Kim et al. 2022) explored the lottery ticket hypothesis with Iterative Magnitude Pruning (IMP) in SNN pruning. (Deng et al. 2021) combined spatio-temporal backpropagation (STBP) and alternating direction method of multipliers (ADMM) and proposed a regularization method based on activity. (Chen et al. 2021) improved the Deep-R method with a weight regeneration mechanism.

However, the binary representation with integrate-and-fire and non-differentiable property of spike signals make training deep SNNs challenging (Zheng et al. 2021; Wu et al. 2019; Shrestha et al. 2021). Spike signals, decided by the membrane potential and the threshold, are easy to be confused by disturbance and suffer from spike vanish or explosion, resulting in insufficient expression of feature information. The non-differentiable property of spikes necessitates surrogate function to approximate gradients and leads to gradient vanishing. The incomplete feature representation and gradient vanishing hinder training SNNs. This challenge becomes particularly prominent the pruned SNNs because it's difficult to retain the most critical parameters from the not fully trained network. The current state-of-the-art (SOTA) methods typically require extended training or iteration times to attain pruned networks, resulting in significant pruning costs(Chen et al. 2021; Kim et al. 2022). The gradient-based rewiring method proposed by (Chen et al. 2021) needs 2048 epochs to prune the 6 convolutional layers SNN. (Kim et al. 2022) spent 2260 epochs for about 90% sparsity and 3100 epochs for about 95% sparsity on VGG-16 and ResNet-19 with lottery hypothesis(LTH) method. (Kim et al. 2022) and (Kim et al. 2023) compressed timesteps during the pruning process to achieve acceleration using KL divergence or temporal information concentration, but this approach introduces new hyperparameters and only yielded acceleration ratios of 1.12 to 1.59. The early-bird algorithm was utilized to prune the network in the early training stages (Kim et al. 2022), but it results in substantial accuracy loss

on the pruned model.

In this paper, inspired by the critical brain hypothesis (Turing 2009), which reveals the critical state of the brain that is highly sensitive to inputs and facilitates information transmission (Kinouchi and Copelli 2006; Beggs 2008; Shew et al. 2009; Beggs and Timme 2012), we aim to obtain the high-efficiency critical pruned networks that maintain the power to extract feature information and keep efficient feedback for different inputs. According to the association between the criticality and the single neuron’s barely-excitable state (Gal and Marom 2013), we propose a metric for neuron criticality and further relate it to the distance between the membrane potential and the threshold voltage with minimal additional computational cost. To obtain the critical pruned model, we design a regeneration mechanism based on neuron criticality to preserve critical neurons during the pruning process. Models through unstructured pruning and regeneration achieve high sparsity (e.g. 95%) with little performance degradation in deep SNNs. We first perform the structured pruning with the regeneration and achieve over 50% Flops reduction. Moreover, we investigate the impact and the underlying mechanisms of our method and find that it efficiently selects potential structures, improves the uniformity of features and reduces the overfitting during the recovery phase.

In summary, our key contributions are as follows:

- Inspired by critical brain hypothesis and criticality research in neuroscience, we propose a metric for neuron criticality of SNNs and design a regeneration mechanism to efficiently obtain the critical pruned network.
- We evaluate our method using VGG-16 and ResNet-19 for unstructured pruning. Our method achieves higher performance compared to SOTA methods with the same time overhead. We also achieve comparable performances (even better on VGG-16) compared to the SOTA method on CIFAR-100 with 11.3x and 15.5x acceleration on 89.91% and 95.69% sparsity.
- We perform the structured pruning using a basic pruning technique and the regeneration mechanism, yielding better results compared to the sophisticated SOTA method. To our knowledge, this is the first work on structured pruning with high flops reduction ($> 50\%$) in deep SNNs.
- We investigate the impact and underlying mechanisms of our method from both experimental and statistical findings. We find that: (1) our method selects critical structures with latent potential which become more important after fine-tuning. (2) Our method improves the uniformity of features within the same class and between the train and test samples and reducing noise. These improve the stability and reduces the overfitting during the recover phrase.

Related Work

Pruning refer to removing specific structures from a network to induce sparsity. Unstructured pruning (Han et al. 2015; Kappel et al. 2015; Ding et al. 2019) removes weight parameters to achieve high level of connection sparsity. However,

common hardware does not fully optimize sparse matrix operations, limiting potential acceleration from unstructured pruning. Structured pruning (He, Zhang, and Sun 2017; He et al. 2019; Lin et al. 2020) achieves structured sparsity by removing entire kernels or channels. This approach is hardware-friendly but might not reach the highest sparsity.

Pruning Criterion The most commonly employed pruning paradigm involves evaluating the impact of structure on network performance through a pruning criterion and subsequently removing the least significant ones. For unstructured pruning, the magnitude of each weight has emerged as the most widespread pruning criterion, which was firstly proposed in (Han et al. 2015) and has seen widespread adoption in pruning for ANNs (Zhu and Gupta 2017; Gale, Elsen, and Hooker 2019; Liu et al. 2021) and SNNs (Neftci et al. 2016; Liu et al. 2019; Kim et al. 2022). The synaptic parameter (Bellec et al. 2018) which represents the connection strength is another pruning criterion. (Chen et al. 2021) improved the synaptic parameter with gradient rewiring and applied it to SNN pruning. For structured pruning, the first and second-order information of the gradient are utilized to design importance scores (Molchanov et al. 2016; He, Zhang, and Sun 2017). (Hu et al. 2016) proposed the average percentage of zeros (APoZs) of the activation layer output serving as a pruning criterion. (Liu et al. 2017) proposed the scalar parameters representing channels’ significance and used the penalty term to push them towards zero during training.

Pruning Schedule The setting of pruning schedules affects the performance of pruned networks. Iterative pruning follows the pruning-fine-tuning pattern with settings such as the pruning ratio in one iteration, pruning interval, and number of iterations. (Zhu and Gupta 2017) proposed a gradual sparse ratio schedule with a unified pruning interval for unstructured pruning and was followed by subsequent studies (Gale, Elsen, and Hooker 2019; Liu et al. 2021). (Molchanov et al. 2016, 2019; Ding et al. 2021) implemented the iterative pruning on channel level. (Frankle and Carbin 2018) proposed the lottery hypothesis with a fixed pruning ratio and a longer pruning interval, while inheriting the surviving parameters of the initial model after each iteration. (Kim et al. 2022) proved the lottery hypothesis in SNN pruning. One-shot pruning refers to achieve the target sparsity once. (You et al. 2019) proposed using the Hamming distance of pruning masks in the early stages of training to determine the pruning time. (Kim et al. 2022) implemented the above method on SNN pruning.

Preliminaries

Spiking Neural Network

The spiking neuron is the fundamental unit of SNNs. A neuron collect signals from other neurons or inputs in a time step, and modulates the membrane potential by these signals. An output spike is generated and delivered to post-synaptic neurons when the membrane potential exceeds the threshold. The commonly used neuron model is Leaky Integrate and Fire(LIF) model (Izhikevich 2003). It is defined

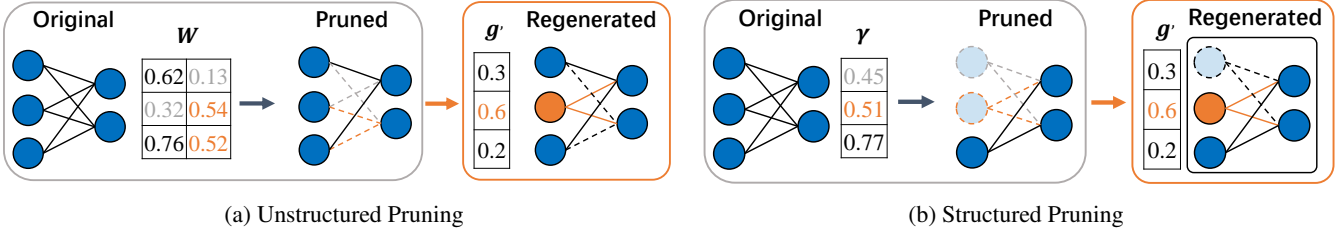


Figure 1: Schematic view of Pruning-Regeneration Process. Faded structures and connections with dotted line are pruned. The gray ones are pruned by basic method mentioned later. The orange ones are extra-pruned (dotted line) and regenerated (solid line) by our method. (a) Unstructured pruning via global magnitude pruning criterion and regeneration based on criticality. (b) Structured pruning via the scaling factor γ (BN layer parameter) and regeneration based on criticality.

as:

$$h[t] = u[t-1] + \frac{1}{\tau} \left(\sum_i w_i s_i[t] - u[t-1] \right) \quad (1)$$

$$u[t] = h[t] \cdot (1 - s[t]) + V_{reset} \cdot s[t] \quad (2)$$

where Eq.1 and Eq.2 describe the charging and resetting processes of a LIF neuron. t represents the current time step. s_i represents the spike train from the i th pre-synaptic neuron and w_i is the corresponding synaptic weight. $u[t]$ denotes the membrane potential at the end of current time step t . V_{reset} represents the reset voltage, which we set to 0. $s[t] \in \{0, 1\}$ represents the output of the neuron in the current time step. The fire process is described as:

$$s[t] = \Theta(h[t] - V_{threshold}) \quad (3a)$$

$$\Theta(x) = 0, x < 0 \text{ otherwise } 1 \quad (3b)$$

where $V_{threshold}$ is the threshold voltage.

For the learning process, we use the spatio-temporal back-propagation (STBP) (Wu et al. 2018) to train SNNs. To overcome the problem that Eq.3b is not differentiable at zero, a surrogate function is commonly used to replace Eq.3b in the backward phase (Wu et al. 2018, 2019; Zheng et al. 2021). Eq.4a defines the surrogate function used in this work. Eq.4b is the derivative function of Eq.4a and is used to approximate the gradient in the backward phase.

$$g(x) = \frac{1}{\pi} \arctan(\pi x) + \frac{1}{2} \quad (4a)$$

$$g'(x) = \frac{1}{1 + \pi^2 x^2} \quad (4b)$$

Criticality in Neuroscience

Neuroscience suggests that the critical state plays a vital role in the brain's efficient information processing (Beggs and Timme 2012; Di Santo et al. 2018). This theory, known as the critical brain hypothesis (Turing 2009), asserts that the brain operates at the critical state. In this state, the brain is highly sensitive to any input that can alter its activity. Even minimal stimuli can trigger a rapid cascade of neuronal excitation, facilitating information transmission throughout the brain (Kinouchi and Copelli 2006; Beggs 2008; Shew et al. 2009; Beggs and Timme 2012).

Previous researches have observed the criticality in neural systems at different scales (Hesse and Gross 2014; Heiney

et al. 2021). Self-organized criticality (SOC) refers to the ability of dynamical systems to effectively tune itself towards the critical state. (Herz and Hopfield 1995) first indicated a mathematical equivalence between SOC models and integrate-and-fire neuron networks. (Gal and Marom 2013) established the association between SOC and single neuron according to the experimental phenomenon. They found that the cortical neurons of newborn rats keep around a barely-excitable state, exhibiting characteristics of SOC. Activities push the neuron towards an excitatory state, while at the longer time scale regulatory feedback pulls it back.

Method

Criticality from Biology to SNNs

Inspired by the critical brain hypothesis, We aim to exploit the advantages of the critical state of brain to improve SNNs. Specifically, we hope that pruned SNNs retain more critical characteristics and maintain sensitivity to inputs and efficiency in feature extraction, ultimately leading to improved post-pruning performance. We start from single neuron to exploit the criticality in SNNs since it shows the lowest level criticality in neuroscience (Gal and Marom 2013). Previous works (Hu et al. 2016; Liu et al. 2022) have improved pruning through properties exhibited by neurons during training and pruning processes. Drawing from these works, a natural idea is to compute the neuron criticality score and select neurons with higher criticality.

The key challenge is to find a suitable metric for neuron criticality. Inspired by (Gal and Marom 2013), we realize the criticality is correlated with the barely-excitable state of neurons. Previous studies (Plessner and Gerstner 2000; Maass 2014) indicate that the magnitude of the membrane potential is positively correlated with the excitation probability. As the membrane potential approaches the threshold voltage, the excitation probability rapidly transitions between 0 and 1. Following this line we propose that neuronal criticality is related to the distance between the membrane potential and the threshold voltage. A neuron's decision is considered to have higher criticality when the membrane potential is closer to the threshold voltage. Considering pruning and training processes, we suggest that the derivative of a surrogate function, such as g' , serves as a suitable criticality metric. It offers several advantages: (1) The derivatives of mainstream surrogate functions reach the highest value when the membrane

potential equals the threshold voltage and rapidly decrease with increasing distance, effectively reflecting the criticality changes of neuron's decisions. (2) The derivative of the surrogate function can be directly obtained during network training with minimal additional computational cost. (3) The derivative of the surrogate function has a unified value range, enabling global ranking and pruning.

Regeneration via Neuron Criticality

We aim to design a compatible method to reserve critical neurons for different pruning strategy. To achieve this, we integrate the criticality metric and a regeneration mechanism of neurons. After each pruning iteration, we reactivate a subset of pruned neurons and their synapses. We re-sort all pruned units in the pruned model based on their criticality scores and reactivate the top k units with the highest scores:

$$S_{new} = S + TopK(C(S')) \quad (5)$$

where S is the set of surviving pruning structures after the pruning iteration. S' is the set of pruned structures. $C(x)$ denotes the criticality score of x .

To compute the criticality score we have

$$s(\mathbf{u}_i) = \text{aggregate}\left(\frac{1}{T} \sum_{i=0}^T g'(\mathbf{u}_i)\right) \quad (6a)$$

$$C(e) = \frac{1}{N} \sum_{i=1}^N s(\mathbf{u}_i) \quad (6b)$$

Eq.6a and 6b illustrate the approach to obtaining criticality scores for a neuron e . \mathbf{u}_i represents the membrane potential array at i th time step. T is the total number of time steps. g'_i is the derivative of surrogate function. N is the total number of sample using to compute the criticality score. $\text{aggregate}()$ represents the way to aggregate the results of the pruning structure. For the fully connected layer, we directly compute the average criticality score for each neuron. For convolutional layers, we explore two approaches: mean aggregation and max aggregation. we finally employ max operation due to its superior performance in the experiments. We suppose the reason is that max aggregation preserves the highest response within the corresponding region, preventing robust responses from being diminished by neighboring elements within the feature map.

Overall Pruning Strategy

So far, we have known how to calculate the criticality scores of neurons. In order to evaluate the impact of preserving critical neurons on sparse SNN, we perform pruning on SNNs at both the unstructured (connection) and structured (channel) levels. As depicted in Figure 1, our approach involves employing the basic pruning techniques while incorporating a regeneration mechanism based on neuron criticality (Implementation details are contained in Appendix A).

Unstructured Pruning To better evaluate the effectiveness of criticality-based regeneration mechanism, we choose the simple global magnitude pruning criterion $|w|$ to achieve

connection level sparsity in deep SNNs, where w is the connection weight. Following the gradual pruning scheme in (Zhu and Gupta 2017), we iteratively prune the network until reaching the target sparsity. After each pruning iteration, we perform regeneration based neuron criticality. To ensure the target sparsity, we expand s_t to s'_t :

$$s'_t = s_t + r(1 - s_t) \quad (7)$$

where r is the regeneration rate and s'_t is the temp sparsity before regeneration at current iteration. We collect the values of $g'(u)$ from the last training iteration before pruning and calculate the average value as the criticality score. We perform the global regeneration after each pruning iteration.

Structured Pruning We employ the scaling factor of the Batch Normalization layer to obtain channel-level sparse models following (Liu et al. 2017). Specifically, We leverage the parameter γ in batch normalization layers as scaling factors and incorporate L1 sparsity regularization during training. After training, we prune channels according to the magnitude of scaling factors. Then we calculate the criticality score for each channel by collecting the average value of derivative of surrogate function from the entire training dataset. Finally we execute regeneration with criticality scores and fine-tune the slimmed network.

Experiment

Experimental Setup

We evaluate our method on two representative architectures VGG-16 (Simonyan and Zisserman 2014) and ResNet-19 (He et al. 2016) for three datasets CIFAR-10, CIFAR-100 (Krizhevsky, Hinton et al. 2009) and Tiny-ImageNet (Hansen 2015). We use SGD optimizer with momentum 0.9 and learning rate 0.3. The batch size is set to 128. We evaluate both unstructured pruning and structured pruning. For unstructured pruning, We set 200 epochs for pruning and 300 epochs for fine-fine for CIFAR-10 and CIFAR-100(50 and 150 for tiny-ImageNet). For structured pruning, we follow (Liu et al. 2017) setting 160 epochs for pre-training and 160 epochs for fine-fine. We set the timestep to 5 for all experiments. Our implementation is based on PyTorch and SpikingJelly (Fang et al. 2020) package. The experiments are executed on an RTX 3090 GPU. More implementation details are contained in Appendix B.

Accuracy and Efficiency Evaluations

Unstructured Pruning We evaluate the performance of our method in Table 1. making comparisons with state-of-the-art methods for both SNNs (Kim et al. 2022) and ANNs (Liu et al. 2021). As a baseline We present the results of GMP (Zhu and Gupta 2017). Our experiments encompass sparsity 90%, 95%, and 98%. The setting of hyperparameters is consistent for all methods. On CIFAR-10, we observe that the performance differences among different methods are relatively small. However, our method still universally improves the performance. On the more complex data CIFAR-100 and Tiny-Imagenet, the performance differences between the methods become more significant,

Dataset Sparsity	CIFAR-10			CIFAR-100			Tiny-ImageNet		
	90%	95%	98%	90%	95%	98%	90%	95%	98%
VGG-16 (Dense)	92.58	-	-	69.35	-	-	55.83	-	-
GMP (Zhu and Gupta 2017)	91.88	92.01	91.61	68.41	68.03	64.76	53.74	53.84	50.11
GraNet (Liu et al. 2021)	91.36	91.04	90.41	68.01	66.84	63.84	53.45	53.38	48.72
LTH-SNN (Kim et al. 2022)	91.73	91.40	90.42	68.29	67.30	64.27	53.72	53.27	50.29
This work	92.34	92.47	91.95	70.20	69.0	65.32	54.94	54.01	50.88
ResNet-19 (Dense)	93.44	-	-	71.33	-	-	58.00	-	-
GMP (Zhu and Gupta 2017)	92.36	92.51	91.67	70.20	69.32	65.49	54.72	54.82	51.71
GraNet (Liu et al. 2021)	92.23	91.85	91.00	68.64	68.09	54.90	54.62	54.80	50.63
LTH-SNN (Kim et al. 2022)	91.94	91.65	90.83	70.47	69.63	65.33	54.94	54.54	51.03
This work	92.69	92.74	91.64	71.21	70.19	65.97	55.48	55.38	52.05

Table 1: Test accuracy of VGG-16 and ResNet19 model after unstructured pruning on CIFAR-10, CIFAR-100 and Tiny-ImageNet. The "Dense" lines show the accuracy of dense models without pruning. We mark the best results in bold. We run the code from (Liu et al. 2021) and (Kim et al. 2022) to obtain results with the same epoch setting.

Model	Method	#Epoch	Top-1(%)	Sparsity
VGG-16	LTH-SNN	2260 (11.3x)	68.90	89.91%
		3100 (15.5x)	68.00	95.69%
	This work	200	69.65	89.91%
			68.60	95.69%
ResNet-19	LTH-SNN	2260 (11.3x)	71.38	89.91%
		3100 (15.5x)	70.45	95.69%
	This work	200	71.36	89.91%
			70.23	95.69%

Table 2: Test accuracy of VGG-16 and ResNet19 models after unstructured pruning on CIFAR-100 with 200 pruning epochs for our method and over 2000 for LTH-SNN (Kim et al. 2022). We compare the results from (Kim et al. 2022) and this work.

and our approach showed a more distinct improvement. It is more interesting that the achievement of our method on the VGG model at 90% sparsity for CIFAR-100, where we obtain accuracy surpassing that of the dense model. This further highlights the effectiveness of the critical model during fine-tune.

In Table 2, we evaluate the efficiency of our method. We compare it with the state-of-the-art work of SNNs(Kim et al. 2022) and observe that while significantly accelerating the pruning with the 11.3-15.5 times speedup, our method maintains comparable performance to the LTH-SNN method. For the VGG-16 model, our method achieve even higher accuracy at sparsity levels of 89.91% and 95.65%.

Structured Pruning In Table 3, we evaluate the performance of our method on CIFAR-100. As pioneers in implementing structured pruning on SNNs, we take the state-of-the-art work of ANNs (Liu et al. 2017; Wang et al. 2021) and

make it portable to SNNs for a comparative analysis. Additionally, we presented (Liu et al. 2017) as our baseline. Our method consistently outperforms Greg (Wang et al. 2021) which is more complex and computationally expensive. Our method also shows significant improvements compared to the baseline, all while maintaining the equivalent level of Flops.

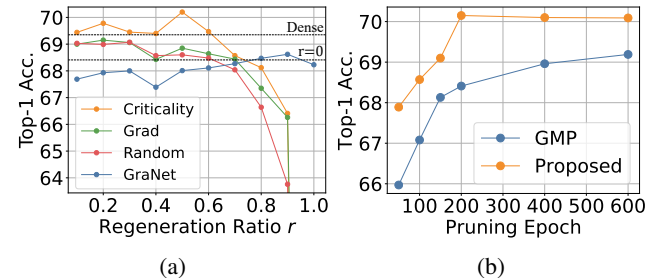


Figure 2: (a) Regeneration method comparison including regeneration based on criticality (ours), gradient, random and GraNet (Liu et al. 2021). The two dashed lines represent the performance of the dense model and $r = 0$ respective. (b) Performance under different pruning epoch setting.

Effect of the Way and Ratio of Regeneration

To evaluate the contributions and robustness of the criticality-based regeneration mechanism, we conduct performance analysis in Figure 2a using different metrics at different regeneration ratio r . The regeneration metrics under evaluation include criticality, grad, random, and GraNet (Liu et al. 2021). Criticality refers to the method based on criticality, Grad employs parameter gradients at the current iteration, Random adopts random ranking, and GraNet represents the GraNet regeneration strategy. The two dashed lines represent the performance of the dense model and $r = 0$ case (GMP) respectively. We observe that all methods exhibited relatively stable performance within the ratio range

Model	Method	Base Top-1(%)	Pruned Top-1(%)	Flops Reduce(%)
VGG-16	(Liu et al. 2017)	69.18	67.92	43.76
	(Wang et al. 2021)	68.81	68.05	43.73
	This work	69.18	68.90	0.28
ResNet-19	(Liu et al. 2017)	72.09	71.08	49.44
	(Wang et al. 2021)	71.34	70.37	49.40
	This work	72.09	71.28	0.81
	(Liu et al. 2017)	72.09	68.34	69.49
	(Wang et al. 2021)	71.34	69.20	69.42
	This work	72.09	70.01	2.08

Table 3: Test accuracy of VGG-16 and ResNet19 models after structured pruning on CIFAR-100. We compare our method to (Liu et al. 2017) and (Wang et al. 2021). We mark the best results in bold.

of 0.1 to 0.6. Criticality, Grad, and Random methods outperform the accuracy when $r = 0$, indicative of their robustness over the wide range of regeneration proportions. In particular, criticality-based regeneration consistently outperforms the Grad and Random regeneration across all ratio settings, even surpassing the performance of the dense model within the 0.1-0.6 proportion range. This highlights the superiority of our method. GraNet exhibits distinct performance dynamics compared to other methods. We attribute this behavior to GraNet’s implementation, which employs cosine decay for the regeneration ratio, gradually diminishing its impact as training progresses.

Effect of Pruning Epoch

To evaluate the sensitivity of our method to pruning cost, we compare the performance of GMP and our work at different pruning epoch settings in Figure 2b. We observe that when the pruning cost is low, our work exhibits a significant performance advantage over GMP. As the cost increases, the performance gradually improves. our method’s performance consistently outperforms GMP and reaches peak around 200, indicating the complete gains from the critical state.

Discussion

In order to investigate the impact and underlying mechanisms of neuron criticality during pruning and fine-tuning, we present the experimental results and statistical findings for the pruned model in this section for more in-depth analysis.

Regeneration Survival In Figure 3a, we show the proportion of weights pruned using magnitude pruning and rescued by the regeneration in each pruning iteration. The regenerated ones consistently account for more than 50% for different sparsity. Furthermore, we separately calculate the proportion of structures survived due to our method in final models through both unstructured and structured

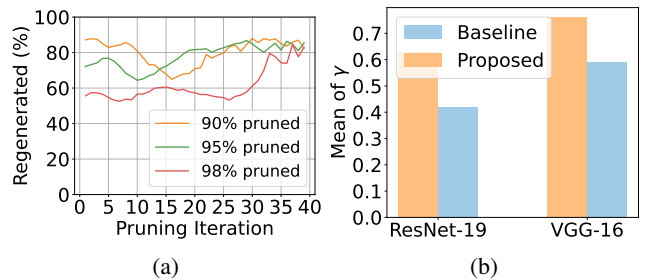


Figure 3: (a) The proportion of weights rescued by the regeneration from magnitude pruning in each pruning iteration. r sets to 0.5, 0.2 and 0.1 for the final sparsity 90%, 95% and 98%. (b) Mean importance of non-overlapping channels between our method and baseline for structured pruning after fine-tuning.

pruning. For the VGG-16 model obtained through unstructured pruning with 90% sparsity, the percentage of structures survived via regeneration is 48.03%. For the ResNet-19 model obtained through structured pruning with 49.46% Flops, the percentage of structures survived via regeneration is 42.60%. This underscores the significant impact of our method on the structure of pruned models.

Importance transition We conduct a comparative analysis of the importance transition in non-overlapping surviving structures between the models obtained using our method and GMP. To better distinguish non-overlapping structures, we focus on the results of structured pruning. In Figure 3b, we present the means of γ (normalized) corresponding to non-overlapping channels in the models through the fine-tuning process with L1 sparsity regularization for two methods. The results show that the channels regenerated by our method exhibit significantly higher importance compared to those without regeneration. Considering that the regenerated channels originally corresponded to lower γ values

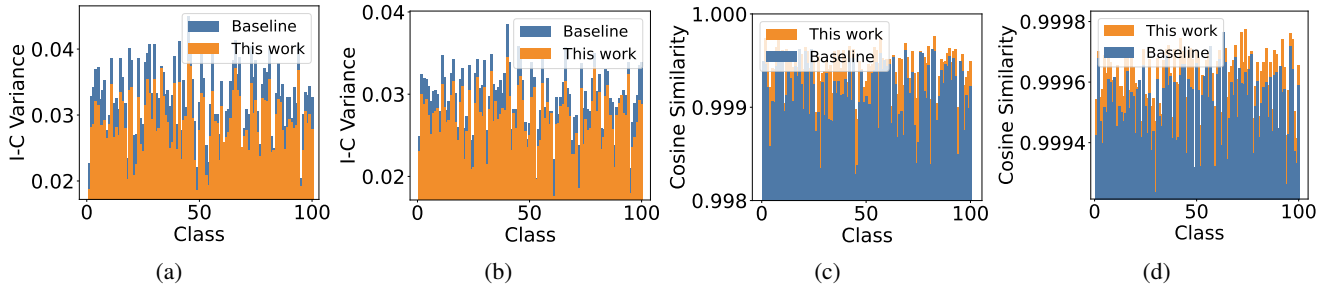


Figure 4: Comparison of the difference in feature extraction of models pruned by our method and GMP. Our method achieves more uniform feature representations. (a) Intra-cluster variance of VGG-16 through unstructured pruning. (b) Intra-cluster variance of ResNet-19 through structured pruning. (c) Cosine similarity of the means of features for each class between the training and test dataset on VGG-16 through unstructured pruning. (d) Cosine similarity of the means of features for each class between the training and test dataset on ResNet-19 through structured pruning.

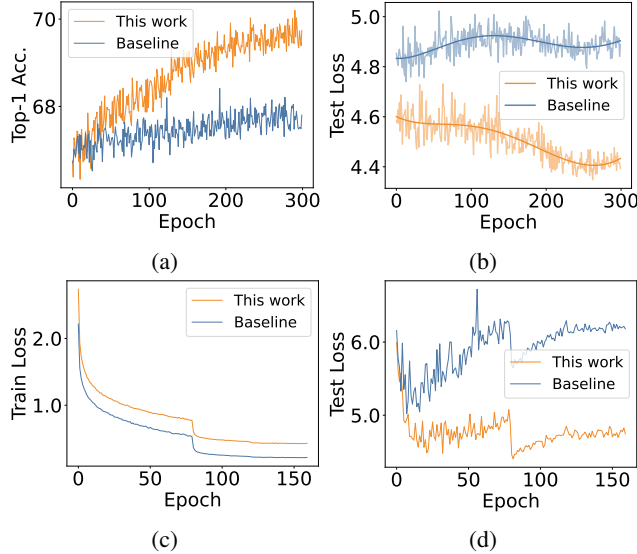


Figure 5: Fine-tune process on VGG-16 after unstructured pruning and ResNet-19 after structured pruning (The complete results are given in Appendix C). (a) Test accuracy on VGG-16. (b) Test loss on VGG-16. (c) Train loss on ResNet-19. (d) Test Loss on ResNet-19.

and higher criticality, this result suggests the following role of our method: (1) Identifying structures with latent potential, thereby taking the pruned model with greater promise. (2) Leveraging the criticality theory, the pruned model benefits from more efficient feedback during fine-tuning, enabling the high-criticality channels to occupy key positions and consequently leading to higher performance gains.

Feature Extraction The critical brain theory suggests that the critical state of the brain promotes feature extraction and transmission. We compare the difference in feature extraction of models pruned by our method and GMP. In Figure 4a and Figure 4b, we show the intra-cluster variance (Kiang 2001) of the features in CIFAR-100 for unstructured pruning and structured pruning, respectively. The intra-cluster vari-

ance measures the compactness of intra-cluster sample representations (Oti et al. 2020). We extract feature maps before the fully connected classifier, and normalize them to eliminate the influence of absolute values. Our model achieved lower variances in almost all classes, indicating enhanced compactness in class features. This improvement is consistent for both unstructured pruning and structured pruning. Furthermore, Figure 4c and Figure 4d illustrate the cosine similarity of the means of features for each class between the training and test dataset. Our model exhibits higher similarity in feature extraction across almost all classes, leading to a more uniform representation of features between the train and test samples and reducing noise.

In Figure 5a and 5b we present curves of test accuracy and loss during the fine-tune phase for VGG-16 through unstructured pruning. In contrast, Figure 5a demonstrates that our model’s test accuracy steadily recovers during retraining, while the GMP model maintains a lower accuracy level with significant fluctuations after an initial brief increase. Figure 5b and 5d show that our model’s test loss steadily decreases, while the baseline model’s test loss initially decreases briefly but then rises. Figure 5c and 5d show that our model exhibits higher training loss but lower test loss comparing to baseline. Combining the above observation, we believe that the baseline models suffer from overfitting during fine-tune and our method reduces this because the critical model learns consistent feature representation and reduce noise between training and test samples.

Conclusion

In this paper, inspired by critical brain hypothesis in neuroscience, we propose a novel neuron criticality metric and design a regeneration based on criticality for SNN pruning. Experimental results demonstrate that our method outperforms previous SNN pruning methods for both unstructured and structured pruning. We keeps comparable performance with SOTA method while significantly reducing pruning cost. Moreover, we investigate the impact and underlying mechanisms of our method and find that it efficiently identifies potential structures, enhances feature uniformity and reduces the overfitting during the recover phase.

Appendix

A. Details of Pruning Strategy

Unstructured Pruning We present the details for the basic pruning method and the regeneration mechanism for unstructured pruning. As mentioned in method section, we choose a global magnitude pruning criterion to achieve connection level sparsity. Specifically, we have:

$$s(w) = |w|, \quad (8)$$

where $s(w)$ is the importance score of w . The gradual pruning scheme from (Zhu and Gupta 2017) is

$$s_t = s_f - s_f \left(1 - \frac{n\Delta t}{T_f}\right)^3, \quad (9)$$

where s_f represents the target sparsity. n is current pruning iteration. T_f is the end point of pruning. Δt is a constant and represents the interval of pruning iterations. We present the overall pruning strategy with regeneration in algorithm 1.

Algorithm 1: The pseudo code of unstructured pruning

Require: target sparsity s_f , pruning interval Δt , end point T_f and regeneration ratio r .
Parameter: Model weights W .

- 1: Let $n \leftarrow 0$.
- 2: **for** each training step t **do**
- 3: TrainOneStep()
- 4: **if** $t < T_f$ and $(t \bmod \Delta t) == 0$ **then**
- 5: $n = n + 1$
- 6: $s_t \leftarrow \text{CurrentSparsity}(s_f, n, T_f, \Delta t)$ \triangleright Eq.9
- 7: $s'_t \leftarrow \text{ExtendSparsity}(s_t, r)$ \triangleright Eq.7
- 8: $W = \text{Pruning}(|W|, s'_t)$ \triangleright Eq.8
- 9: $C(W) \leftarrow \text{Criticality}((u_{\text{currentStep}}))$ \triangleright Eq.6
- 10: $W = \text{Regeneration}(C(W), s'_t - s_t)$ \triangleright Eq.5
- 11: **end if**
- 12: **end for**

Algorithm 2: The pseudo code of structured pruning

Require: target sparsity s_t , and regeneration ratio r .
Parameter: Model channels chs and scaling factor set Γ .

Train process:

- 1: Train model with L1 sparsity regularization. \triangleright Ep.10

Pruning and Regeneration:

- 2: $s'_t \leftarrow \text{ExtendSparsity}(s_t, r)$ \triangleright Eq.7
- 3: $chs = \text{Pruning}(chs, s'_t, |\Gamma|)$ \triangleright pruning by $|\Gamma|$
- 4: $C(chs) \leftarrow \text{Criticality}((u_{\text{trainSet}}))$ \triangleright Eq.6
- 5: $chs = \text{Regeneration}(C(chs), s'_t - s_t)$ \triangleright Eq.5

Fine-tuning process:

- 6: Fine-tuning model without L1 sparsity regularization.

Structured Pruning Following the approach proposed by (Liu et al. 2017), we have a scaling factor for each channel and jointly train these scaling factors with sparsity regularization:

$$L = \sum_{(x,y)} l(f(x, W), y) + \lambda \sum_{\gamma \in \Gamma} |\gamma|, \quad (10)$$

where (x, y) is the input and target pair. W is network weights. The first sum-term denotes train loss in the backward process. γ is the scaling factor defined as the factor parameter of linear mapping in batch normalization layer. The second sum-term is the L1 sparsity regularization.

We present the overall pruning strategy with regeneration in algorithm 2.

B. Experiment Details

The global settings of hyperparameters of experiments are illustrated in Table 4. Table 5 and 6 respectively illustrate settings for unstructured pruning and structured pruning. To be consistent with previous works, we use step lr scheduler for structured pruning and cosine lr scheduler for unstructured pruning.

Parameter	Description	Value
Batch Size	-	128
Optimizer	-	SGD
<i>momentum</i>	-	0.9
<i>lr</i>	Learning Rate	0.3
<i>T</i>	# Timestep	5
τ	Membrane Constant	4/3
$V_{\text{threshold}}$	Threshold Voltage	1.0
V_{reset}	Reset Voltage	0.0

Table 4: Global settings of hyperparameters for all experiments.

Dataset	CIFAR-10/100	Tiny-ImageNet
N_p	200	50
N_f	300	100
wd	5e-4	5e-4
Δt	2000	1000
s_f	[0.90, 0.95, 0.98]	[0.90, 0.95, 0.98]
r	[0.5, 0.2, 0.1]	[0.3, 0.1, 0.05]

Table 5: Experiment hyperparameters of unstructured pruning for VGG-16 and ResNet-19 on CIFAR-10, CIFAR-100 and Tiny-ImageNet. Pruning Epochs (N_p), Fine-tuning Epochs after pruning (N_f), Weight decay (wd), pruning interval (Δt), Final sparsity s_f , Regeneration radio (r). The settings are common for VGG-16 and ResNet-19.

C. Model Curves during Fine-tuning

In Figure 6 and 7, we present complete curves of accuracy and loss during the fine-tune phase for VGG-16 through unstructured pruning and for ResNet-19 through structured pruning. As mentioned in discussion section, Figure 6c and 7c demonstrates our model recovers better during fine-tuning. The comparison between curves of training and test indicates our contribution to reduce overfitting.

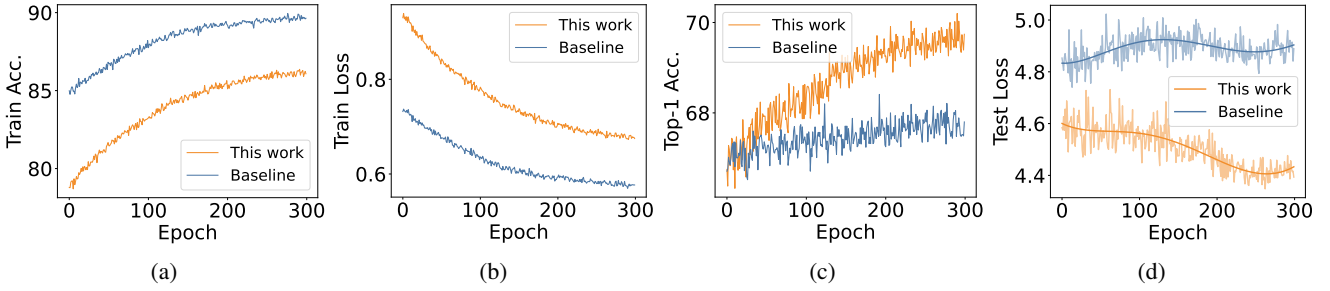


Figure 6: Fine-tune process on VGG-16 after unstructured pruning. (a) Train accuracy. (b) Train loss. (c) Test accuracy. (d) Test Loss.

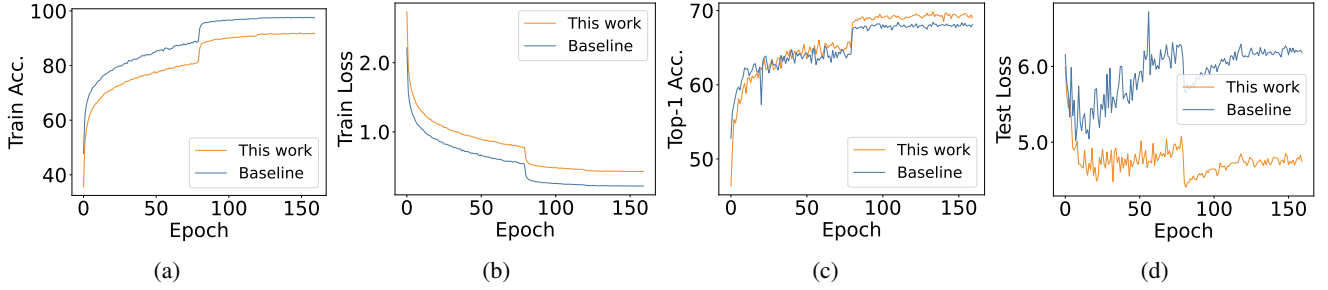


Figure 7: Fine-tune process on ResNet-19 after structured pruning. (a) Train accuracy. (b) Train loss. (c) Test accuracy. (d) Test Loss.

Model	VGG-16	ResNet-19
N_t	160	160
N_f	160	160
N_1, N_2	[80, 120]	[80, 120]
s	1e-4	1e-4
perecent ¹	[0.4522, 0.6764]	[0.512, 0.658]
r	[0.1, 0.05]	[0.3, 0.1]

¹ Choosing the the special values to achieve the same flops reducing with SOTA for fair comparison.

Table 6: Experiment hyperparameters of structured pruning for VGG-16 and ResNet-19 on CIFAR-100. Training Epochs with L1 sparsity regularization (N_t), Fine-tuning Epochs after pruning (N_f), lr Drop (10x) Epochs (N_1, N_2), Target sparsity s_t (perecent), Regeneration radio (r).

References

Akopyan, F.; Sawada, J.; Cassidy, A.; Alvarez-Icaza, R.; Arthur, J.; Merolla, P.; Imam, N.; Nakamura, Y.; Datta, P.; Nam, G.-J.; et al. 2015. Truenorth: Design and tool flow of a 65 mw 1 million neuron programmable neurosynaptic chip. *IEEE transactions on computer-aided design of integrated circuits and systems*, 34(10): 1537–1557.

Beggs, J. M. 2008. The criticality hypothesis: how local cortical networks might optimize information processing. *Philosophical Transactions of the Royal Society A: Mathematical, Physical and Engineering Sciences*, 366(1864): 329–343.

Beggs, J. M.; and Timme, N. 2012. Being critical of criticality in the brain. *Frontiers in physiology*, 3: 163.

Bellec, G.; Salaj, D.; Subramoney, A.; Legenstein, R.; and Maass, W. 2018. Long short-term memory and learning-to-learn in networks of spiking neurons. *Advances in neural information processing systems*, 31.

Chen, Y.; Yu, Z.; Fang, W.; Huang, T.; and Tian, Y. 2021. Pruning of Deep Spiking Neural Networks through Gradient Rewiring. In Zhou, Z.-H., ed., *Proceedings of the Thirtieth International Joint Conference on Artificial Intelligence, IJCAI-21*, 1713–1721. International Joint Conferences on Artificial Intelligence Organization. Main Track.

Davies, M.; Srinivasa, N.; Lin, T.-H.; Chinya, G.; Cao, Y.; Choday, S. H.; Dimou, G.; Joshi, P.; Imam, N.; Jain, S.; et al. 2018. Loihi: A neuromorphic manycore processor with on-chip learning. *Ieee Micro*, 38(1): 82–99.

Deng, L.; Wu, Y.; Hu, Y.; Liang, L.; Li, G.; Hu, X.; Ding, Y.; Li, P.; and Xie, Y. 2021. Comprehensive snn compression using admm optimization and activity regularization. *IEEE transactions on neural networks and learning systems*.

Di Santo, S.; Villegas, P.; Burioni, R.; and Muñoz, M. A. 2018. Landau–Ginzburg theory of cortex dynamics: Scale-free avalanches emerge at the edge of synchronization. *Proceedings of the National Academy of Sciences*, 115(7): E1356–E1365.

Ding, X.; Hao, T.; Tan, J.; Liu, J.; Han, J.; Guo, Y.; and Ding, G. 2021. Resrep: Lossless cnn pruning via decoupling re-

membering and forgetting. In *Proceedings of the IEEE/CVF International Conference on Computer Vision*, 4510–4520.

Ding, X.; Zhou, X.; Guo, Y.; Han, J.; Liu, J.; et al. 2019. Global sparse momentum sgd for pruning very deep neural networks. *Advances in Neural Information Processing Systems*, 32.

Fang, W.; Chen, Y.; Ding, J.; Chen, D.; Yu, Z.; Zhou, H.; Masquelier, T.; Tian, Y.; and other contributors. 2020. SpikingJelly. <https://github.com/fangwei123456/spikingjelly>. Accessed: 2022-5-1.

Frankle, J.; and Carbin, M. 2018. The lottery ticket hypothesis: Finding sparse, trainable neural networks. *arXiv preprint arXiv:1803.03635*.

Gal, A.; and Marom, S. 2013. Self-organized criticality in single-neuron excitability. *Physical Review E*, 88(6): 062717.

Gale, T.; Elsen, E.; and Hooker, S. 2019. The state of sparsity in deep neural networks. *arXiv preprint arXiv:1902.09574*.

Han, S.; Pool, J.; Tran, J.; and Dally, W. 2015. Learning both weights and connections for efficient neural network. *Advances in neural information processing systems*, 28.

Hansen, L. 2015. Tiny ImageNet challenge submission. *CS 231N*, 5.

He, K.; Zhang, X.; Ren, S.; and Sun, J. 2016. Deep residual learning for image recognition. In *Proceedings of the IEEE conference on computer vision and pattern recognition*, 770–778.

He, Y.; Liu, P.; Wang, Z.; Hu, Z.; and Yang, Y. 2019. Filter pruning via geometric median for deep convolutional neural networks acceleration. In *Proceedings of the IEEE/CVF conference on computer vision and pattern recognition*, 4340–4349.

He, Y.; Zhang, X.; and Sun, J. 2017. Channel pruning for accelerating very deep neural networks. In *Proceedings of the IEEE international conference on computer vision*, 1389–1397.

Heiney, K.; Huse Ramstad, O.; Fiskum, V.; Christiansen, N.; Sandvig, A.; Nichelle, S.; and Sandvig, I. 2021. Criticality, connectivity, and neural disorder: a multifaceted approach to neural computation. *Frontiers in computational neuroscience*, 15: 611183.

Herz, A. V.; and Hopfield, J. J. 1995. Earthquake cycles and neural reverberations: collective oscillations in systems with pulse-coupled threshold elements. *Physical review letters*, 75(6): 1222.

Hesse, J.; and Gross, T. 2014. Self-organized criticality as a fundamental property of neural systems. *Frontiers in systems neuroscience*, 8: 166.

Hu, H.; Peng, R.; Tai, Y.-W.; and Tang, C.-K. 2016. Network trimming: A data-driven neuron pruning approach towards efficient deep architectures. *arXiv preprint arXiv:1607.03250*.

Izhikevich, E. M. 2003. Simple model of spiking neurons. *IEEE Transactions on neural networks*, 14(6): 1569–1572.

Kappel, D.; Habenschuss, S.; Legenstein, R.; and Maass, W. 2015. Network plasticity as Bayesian inference. *PLoS computational biology*, 11(11): e1004485.

Kiang, M. Y. 2001. Extending the Kohonen self-organizing map networks for clustering analysis. *Computational Statistics & Data Analysis*, 38(2): 161–180.

Kim, Y.; Li, Y.; Park, H.; Venkatesha, Y.; Hambitzer, A.; and Panda, P. 2023. Exploring temporal information dynamics in spiking neural networks. In *Proceedings of the AAAI Conference on Artificial Intelligence*, volume 37, 8308–8316.

Kim, Y.; Li, Y.; Park, H.; Venkatesha, Y.; Yin, R.; and Panda, P. 2022. Exploring lottery ticket hypothesis in spiking neural networks. In *Computer Vision–ECCV 2022: 17th European Conference, Tel Aviv, Israel, October 23–27, 2022, Proceedings, Part XII*, 102–120. Springer.

Kinouchi, O.; and Copelli, M. 2006. Optimal dynamical range of excitable networks at criticality. *Nature physics*, 2(5): 348–351.

Krizhevsky, A.; Hinton, G.; et al. 2009. Learning multiple layers of features from tiny images.

Kundu, S.; Datta, G.; Pedram, M.; and Beerel, P. A. 2021. Spike-thrift: Towards energy-efficient deep spiking neural networks by limiting spiking activity via attention-guided compression. In *Proceedings of the IEEE/CVF Winter Conference on Applications of Computer Vision*, 3953–3962.

Lin, M.; Ji, R.; Wang, Y.; Zhang, Y.; Zhang, B.; Tian, Y.; and Shao, L. 2020. Hrank: Filter pruning using high-rank feature map. In *Proceedings of the IEEE/CVF conference on computer vision and pattern recognition*, 1529–1538.

Liu, F.; Zhao, W.; Chen, Y.; Wang, Z.; and Dai, F. 2022. Dynsnn: A dynamic approach to reduce redundancy in spiking neural networks. In *ICASSP 2022-2022 IEEE International Conference on Acoustics, Speech and Signal Processing (ICASSP)*, 2130–2134. IEEE.

Liu, S.; Chen, T.; Chen, X.; Atashgahi, Z.; Yin, L.; Kou, H.; Shen, L.; Pechenizkiy, M.; Wang, Z.; and Mocanu, D. C. 2021. Sparse training via boosting pruning plasticity with neuroregeneration. *Advances in Neural Information Processing Systems*, 34: 9908–9922.

Liu, Y.; Qian, K.; Hu, S.; An, K.; Xu, S.; Zhan, X.; Wang, J.; Guo, R.; Wu, Y.; Chen, T.-P.; et al. 2019. Application of deep compression technique in spiking neural network chip. *IEEE transactions on biomedical circuits and systems*, 14(2): 274–282.

Liu, Z.; Li, J.; Shen, Z.; Huang, G.; Yan, S.; and Zhang, C. 2017. Learning Efficient Convolutional Networks Through Network Slimming. In *Proceedings of the IEEE International Conference on Computer Vision (ICCV)*.

Maass, W. 1997. Networks of spiking neurons: the third generation of neural network models. *Neural networks*, 10(9): 1659–1671.

Maass, W. 2014. Noise as a resource for computation and learning in networks of spiking neurons. *Proceedings of the IEEE*, 102(5): 860–880.

Molchanov, P.; Mallya, A.; Tyree, S.; Frosio, I.; and Kautz, J. 2019. Importance estimation for neural network pruning.

In *Proceedings of the IEEE/CVF conference on computer vision and pattern recognition*, 11264–11272.

Molchanov, P.; Tyree, S.; Karras, T.; Aila, T.; and Kautz, J. 2016. Pruning convolutional neural networks for resource efficient inference. *arXiv preprint arXiv:1611.06440*.

Neftci, E. O.; Pedroni, B. U.; Joshi, S.; Al-Shedivat, M.; and Cauwenberghs, G. 2016. Stochastic synapses enable efficient brain-inspired learning machines. *Frontiers in neuroscience*, 10: 241.

Oti, E. U.; Unyeagu, S.; Nwankwo, C. H.; Alvan, W. K.; and Osuji, G. A. 2020. New K-means clustering methods that minimize the total intra-cluster variance. *Afr. J. Math. Stat. Stud.*, 3: 42–54.

Pei, J.; Deng, L.; Song, S.; Zhao, M.; Zhang, Y.; Wu, S.; Wang, G.; Zou, Z.; Wu, Z.; He, W.; et al. 2019. Towards artificial general intelligence with hybrid Tianjic chip architecture. *Nature*, 572(7767): 106–111.

Plessner, H. E.; and Gerstner, W. 2000. Noise in integrate-and-fire neurons: from stochastic input to escape rates. *Neural computation*, 12(2): 367–384.

Qi, Y.; Shen, J.; Wang, Y.; Tang, H.; Yu, H.; Wu, Z.; Pan, G.; et al. 2018. Jointly learning network connections and link weights in spiking neural networks. In *IJCAI*, 1597–1603.

Roy, K.; Jaiswal, A.; and Panda, P. 2019. Towards spike-based machine intelligence with neuromorphic computing. *Nature*, 575(7784): 607–617.

Shew, W. L.; Yang, H.; Petermann, T.; Roy, R.; and Plenz, D. 2009. Neuronal avalanches imply maximum dynamic range in cortical networks at criticality. *Journal of neuroscience*, 29(49): 15595–15600.

Shrestha, A.; Fang, H.; Rider, D. P.; Mei, Z.; and Qiu, Q. 2021. In-hardware learning of multilayer spiking neural networks on a neuromorphic processor. In *2021 58th ACM/IEEE Design Automation Conference (DAC)*, 367–372. IEEE.

Simonyan, K.; and Zisserman, A. 2014. Very deep convolutional networks for large-scale image recognition. *arXiv preprint arXiv:1409.1556*.

Turing, A. M. 2009. *Computing machinery and intelligence*. Springer.

Wang, H.; Qin, C.; Zhang, Y.; and Fu, Y. 2021. Neural Pruning via Growing Regularization. In *International Conference on Learning Representations (ICLR)*.

Wu, Y.; Deng, L.; Li, G.; Zhu, J.; and Shi, L. 2018. Spatio-temporal backpropagation for training high-performance spiking neural networks. *Frontiers in neuroscience*, 12: 331.

Wu, Y.; Deng, L.; Li, G.; Zhu, J.; Xie, Y.; and Shi, L. 2019. Direct training for spiking neural networks: Faster, larger, better. In *Proceedings of the AAAI conference on artificial intelligence*, volume 33, 1311–1318.

You, H.; Li, C.; Xu, P.; Fu, Y.; Wang, Y.; Chen, X.; Baraniuk, R. G.; Wang, Z.; and Lin, Y. 2019. Drawing early-bird tickets: Towards more efficient training of deep networks. *arXiv preprint arXiv:1909.11957*.

Zheng, H.; Wu, Y.; Deng, L.; Hu, Y.; and Li, G. 2021. Going deeper with directly-trained larger spiking neural networks. In *Proceedings of the AAAI conference on artificial intelligence*, volume 35, 11062–11070.

Zhu, M.; and Gupta, S. 2017. To prune, or not to prune: exploring the efficacy of pruning for model compression. *arXiv preprint arXiv:1710.01878*.